Precision Engineering xxx (2011) xxx–xxx

Contents lists available at SciVerse ScienceDirect

Precision Engineering

journal homepage: www.elsevier.com/locate/precision

Prediction of machining accuracy degradation of machine tools

Kuang-Chao Fan [a,*], Hsi-Ming Chen [a], Tzu-Hsin Kuo [b]

[a] Department of Mechanical Engineering, National Taiwan University, Taiwan
[b] Mechanical and System Research Laboratory, Industrial Technology Research Institute, Taiwan

ARTICLE INFO

Article history:
Received 26 February 2011
Received in revised form 2 November 2011
Accepted 13 November 2011
Available online xxx

Keywords:
Machine tool
Accuracy degradation
Slide-guideway
Contact deformation
Wear

ABSTRACT

Machine tool has to maintain its accuracy for quality control of products. After a long period of cutting operations, obvious wear will occur on the contact surfaces of the slide and the guideway. Such a wear will degrade the accuracy of machine tool due to the increase of Abbé errors. This research proposes a mathematical model so that, at given cutting forces and parameters of the slide-guideway, it is able to calculate the geometric errors of the slide due to contact deformation caused by the wear of the guideway and then predict the positioning errors after a long-term operation. Cutting forces applied to the worktable will cause reaction forces on contact surfaces between the slide and the guideway. Such reaction forces can be solved by static equilibrium equations of deformed free-body diagram of the slide. The induced abrasive wear can then be estimated. A simulation study on a heavy duty machine tool with slide-guideway will show the magnitude of wear on the sliding surface and the consequently caused geometric errors of the moving axis. Experimental tests show that, if modifying the wear coefficient to a function of sliding distance, the analytical result is in good agreement with the experimental result.

1. Introduction

The accuracy of a machined part depends on the machining accuracy of the machine tool. Although the machining accuracy meets the specifications while the machine tool is new, it is unable to guarantee that the accuracy still maintains at the acceptable tolerance range after a long-term operation. Positioning errors are dynamically related to the errors of the working stage, cutting forces induced errors, tool wear, slide-guideway wear, ambient temperature, vibration, etc. Wear of the slide-guideway will gradually increase during machining operations.

Regarding the theory of wear, Burwell and Strang [1] classified the wear behaviors to abrasive wear, adhesive wear, erosive wear, fretting wear, corrosive wear and fatigue wear. Archard and Hirst [2] assumed that the volume of material removed by wear is proportional to the interface pressure, sliding distance and wear coefficient. Many papers investigated the wear of contact components by Archard equation, but rarely studied the machine tool slide-guideway wear.

In the past, many researchers measured the contact pressures between the slide and guideway mostly by experiments. Masuko and Ito [3] analyzed contact pressure distribution on the slide-guideway under mixed lubrication condition by the use of ultrasonic wave method. Furukawa and Moronuki [4] analyzed the contact deformation of a machine tool slide-guideway and its effect on the machining accuracy. They proposed a design policy to minimize the machining error by obtaining three-dimensional displacement of the slide caused by contact deformation. Hinduja [5] and Back [6] investigated the deformation and pressure distribution in the joints by FEM. They developed a hydrostatic plate and spring system for modeling the contact between the fixed and sliding joints.

This research proposes a mathematical model so that, given known cutting forces and parameters of slide-guideway, it can calculate the geometric errors of slide due to contact deformation and the positioning errors caused by wear of the guideway after a long-term operation. Cutting forces applied to the worktable will cause surface deformation of the slide-guideway. Reaction forces on contact surfaces between slide and guideway can be formulated by using homogeneous transformation matrix and multiple integration method. All contact forces can be obtained by solving the static equilibrium equations of the slide. Force induced abrasive wear can then be estimated. Case study on a heavy duty machine tool with slide-guideway will show the magnitude of wear on the sliding surface and the consequently caused geometrical errors of the moving slide.

2. Contact deformation of slide-guideway

Cutting force, feed force and friction force applied to the slide will yield surface deformation of the slide-guideway and cause five

* Corresponding author at: Department of Mechanical Engineering, National Taiwan University, Taipei City 10617, Taiwan.
E-mail address: fan@ntu.edu.tw (K.-C. Fan).

0141-6359/$ – see front matter © 2011 Elsevier Inc. All rights reserved.
doi:10.1016/j.precisioneng.2011.11.002

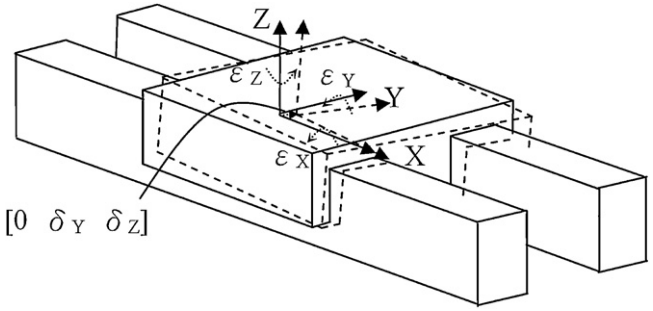

Fig. 1. Geometric errors of the slide.

geometric errors of the slide, namely two straightness errors (δ_Y, δ_Z) and three angular errors (ε_X, ε_Y, ε_Z), as shown in Fig. 1.

Considering the deformation between two contact surfaces, the compressed volume can be represented by the shadow area in Fig. 2. The deformed volume can be described as the enclosed space between two contact surfaces and two side faces, and it can be calculated by multiple integration method.

Surface compliance within the range of mean interface pressure of machine tool slide-guideway has been analyzed based on the experimental data to describe the relationship between the normal pressure (P) and the deformation (λ) of the surfaces [7–12].

$$\lambda = cP^m \tag{1}$$

where λ is normal deformation (in μm), P is normal pressure (kgf/cm^2), c is coefficient of normal contact flexibility, and m is coefficient of non-linearity of deformations. c and m are determined by experiments, their values are dependent on the type of material and the condition of the contact surfaces.

2.1. Mathematical models of a single contact surface

The single contact surface model is shown in Fig. 3. The origin of coordinate system 0 is located at the center of the slide. The three explicit corner points of the slide, marked by three small red circles, are selected as the reference points. This system is used to derive the following mathematical model of the slide-guideway.

External cutting forces applied to the slide will cause surface deformation of the slide-guideway yielding to slight slide geometric errors. When the deformation occurs the slide will be shifted by (δ_{y0}, δ_{z0}) due to straightness errors, and rotated by (ε_{x0}, ε_{y0}, ε_{z0}) due to angular errors. The coordinate system 1 is located at the center of the deformed slide and its three axes are parallel to the sides of the deformed slide respectively, as shown in Fig. 3. The coordinate system 2 is located at the center of the contact surface, and its three axes are parallel to the sides of the guideway respectively. It is seen that coordinate system 2 is related to coordinate system 0 through the translation by half of the height ($-d$) in Z-axis and rotation by 180° in Y-axis of coordinate system 0. The original reference points are embedded into the deformed volume, as indicated by dashed circles in Fig. 3. The compressed volume is represented by the shadow area.

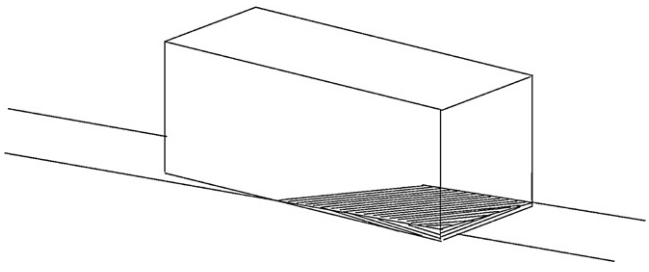

Fig. 2. Volume of deformation (shadow part).

The homogeneous transform matrix (HTM) of coordinate system 0 to coordinate system 1 is expressed by

$$ {}^0T_1 = \begin{bmatrix} 1 & -\varepsilon_{Z0} & \varepsilon_{Y0} & 0 \\ \varepsilon_{Z0} & 1 & -\varepsilon_{X0} & \delta_{Y0} \\ -\varepsilon_{Y0} & \varepsilon_{X0} & 1 & \delta_{Z0} \\ 0 & 0 & 0 & 1 \end{bmatrix} \tag{2}$$

The HTM of coordinate system 0 to coordinate system 2 is

$$ {}^2T_0 = \begin{bmatrix} 1 & 0 & 0 & 0 \\ 0 & 1 & 0 & 0 \\ 0 & 0 & 1 & -d \\ 0 & 0 & 0 & 1 \end{bmatrix} \cdot \begin{bmatrix} cos(\pi) & 0 & \sin(\pi) & 0 \\ 0 & 1 & 0 & 0 \\ -\sin(\pi) & 0 & \cos(\pi) & 0 \\ 0 & 0 & 0 & 1 \end{bmatrix} = \begin{bmatrix} \cos(\pi) & 0 & \sin(\pi) & 0 \\ 0 & 1 & 0 & 0 \\ -\sin(\pi) & 0 & \cos(\pi) & -d \\ 0 & 0 & 0 & 1 \end{bmatrix} \tag{3}$$

The HTM of coordinate system 1 to coordinate system 2 can thus be obtained

$$ {}^2T_1 = {}^2T_0 \cdot {}^0T_1 \tag{4}$$

It yields to

$$ {}^2T_1 = \begin{bmatrix} -1 & \varepsilon_{Z0} & -\varepsilon_{Y0} & 0 \\ \varepsilon_{Z0} & 1 & -\varepsilon_{X0} & \delta_{Y0} \\ \varepsilon_{Y0} & -\varepsilon_{Z0} & -1 & -d-\delta_Z \\ 0 & 0 & 0 & 1 \end{bmatrix} \tag{5}$$

The surface equation of the deformed slide can be represented by the plane containing three reference points in coordinate system 1 ($X_{(1)}$, $Y_{(1)}$, $Z_{(1)}$), as shown in Fig. 3. Since the deformed volume is to be calculated in coordinate system 2 ($X_{(2)}$, $Y_{(2)}$, $Z_{(2)}$), these reference points have to be expressed by this coordinate. Eq. (6) shows the locations of these points in coordinate system 2 transformed from coordinate system 1.

$$ \begin{bmatrix} X_{(2)} \\ Y_{(2)} \\ Z_{(2)} \\ 1 \end{bmatrix} = {}^2T_1 \cdot \begin{bmatrix} X_{(1)} \\ Y_{(1)} \\ Z_{(1)} \\ 1 \end{bmatrix} = \begin{bmatrix} -X_{(1)} - Z_{(1)} \cdot \varepsilon_{Y0} + Y_{(1)} \cdot \varepsilon_{Z0} \\ Y_{(1)} + \delta_{Y0} - Z_{(1)} \cdot \varepsilon_{X0} + X_{(1)} \cdot \varepsilon_{Z0} \\ -d - Z_{(1)} - \delta_{Z0} - Y_{(1)} \cdot \varepsilon_{X0} + X_{(1)} \cdot \varepsilon_{Y0} \\ 1 \end{bmatrix} \tag{6}$$

The equation of the bottom surface of deformed volume can be derived by these three reference points, as expressed by Eq. (7) in which n_{X2}, n_{Y2}, and n_{Z2} are the x, y, and z components of the normal vector of the bottom surface n_2, and $[X_{1(2)}\, Y_{1(2)}\, Z_{1(2)}]^T$ is any point of the three reference points. The normal vector of surface n_2 can be derived from cross product of two vectors which are calculated by three reference points.

$$Z_{(2)} = \frac{n_{X2}(X_{(2)} - X_{1(2)}) + n_{Y2}(Y_{(2)} - Y_{1(2)})}{-n_{Z2}} + Z_{1(2)} \tag{7}$$

The deformed volume can be calculated by multiple integration method, as shown in Fig. 4. For clarity in view, Z_2 axis is directed upward. Fig. 5 plots a cross-sectional view showing the contact line. The deformed volume of the slide (V_1) is the zone above the X_2Y_2 plane and the non-deformed volume (V_2) is the zone below X_2Y_2 plane. Let the volume corresponding to the infinitesimal area δA be δV, i.e.

$$\delta V = f(\delta_{Y0}, \delta_{Z0}, \varepsilon_{X0}, \varepsilon_{Y0}, \varepsilon_{Z0}, X_{(2)}, Y_{(2)}) = Z_{(2)}\delta A \tag{8}$$

It is seen that δV is bound by the reference plane and the contact surface. It is a function of five geometrical errors of the slide. The

Please cite this article in press as: Fan K-C, et al. Prediction of machining accuracy degradation of machine tools. Precis Eng (2011), doi:10.1016/j.precisioneng.2011.11.002

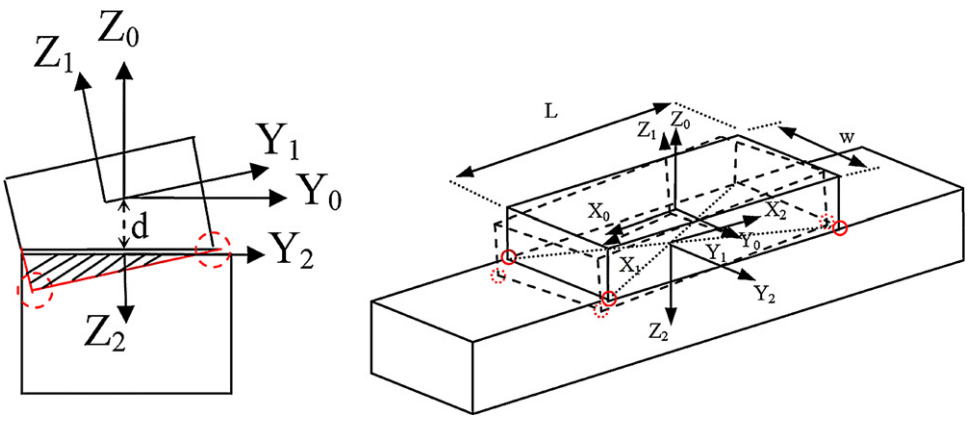

Fig. 3. Coordinate systems and three reference points.

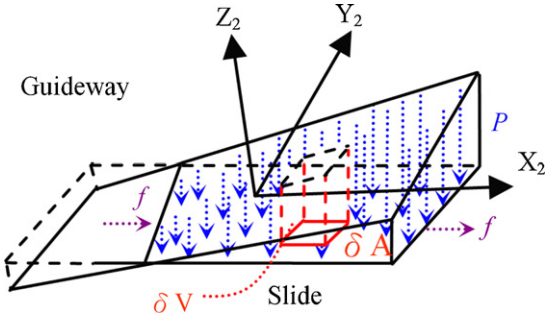

Fig. 4. Deformed volume by multiple integration method.

integration of δV across entire X_2Y_2 plane contains both V_1 and V_2 volumes but in different signs, i.e.

$$\int_{-Y_{(2)}}^{Y_{(2)}}\int_{-X_{(2)}}^{X_{(2)}} \delta V\, dX_{(2)}\, dY_{(2)} = V_1 - V_2$$

Alternatively, the integration of $|\delta V|$ will result in $(V_1 + V_2)$. Hence, the total deformed volume can be found as

$$V_1 = \frac{\int_{-Y_{(2)}}^{Y_{(2)}}\int_{-X_{(2)}}^{X_{(2)}} |\delta V|\, dX_{(2)}\, dY_{(2)}}{2} + \frac{\int_{-Y_{(2)}}^{Y_{(2)}}\int_{-X_{(2)}}^{X_{(2)}} \delta V\, dX_{(2)}\, dY_{(2)}}{2} \quad (9)$$

As given in Fig. 3, the slide's contact face has length L and width w, so the bounds of $X_{(2)}$ and $Y_{(2)}$ correspond to $L/2$ and $w/2$ respectively.

From Eq. (1) it is known that the amount of surface deformation is dependent on the contact pressure. Here, the normal deformation at point $(X_{(2)}, Y_{(2)})$ is the same as $Z_{(2)}$ of Eq. (7). According to the material property of Turcite B [15], the normal deformation can be assumed linear to the contact pressure. Therefore, setting c to be $1/K$ and m to be 1, the contact pressure is expressed by

$$P = Z_{(2)} \cdot K \quad (10)$$

The reaction force (R) at contact surface is the area integration of contact pressure P, and the friction force (f) is μR, where μ is the friction coefficient.

$$R = \iint (P\delta A)dA = \iint \delta V \cdot K\, dA = KV_1 \quad (11)$$

The moment around the X-axis can be expressed by

$$M_{RX} = \iint (P\delta A)y\ dA = K \iint \delta V y\, dA \quad (12)$$

It is clearly seen that external cutting forces and feed force applied to the slide will cause surface deformation of the slide and guideway yielding to geometric errors of the slide. The reaction forces and moments on the contact surfaces are derived from the deformed volume which is a function of δ_{Y0}, δ_{Z0}, ε_{X0}, ε_{Y0} and ε_{Z0}.

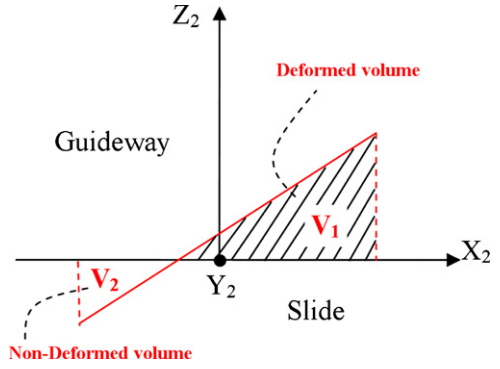

Fig. 5. Definition of deformed volume.

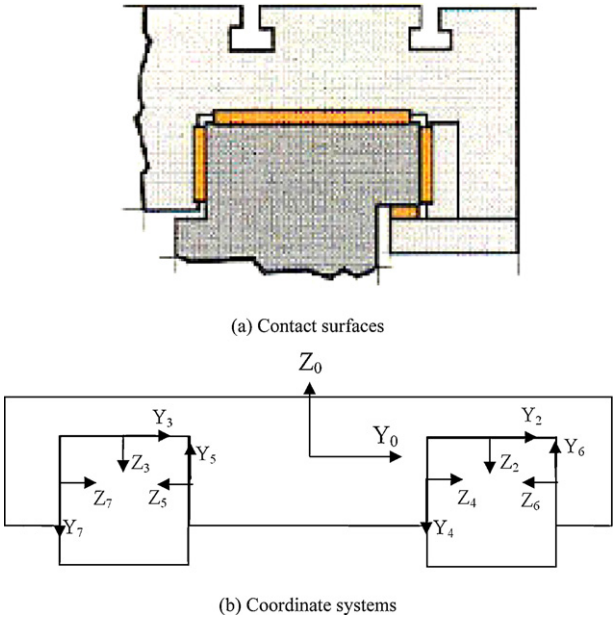

Fig. 6. Machine tool slide-guideway, (a) contact surfaces and (b) coordinate systems.

Please cite this article in press as: Fan K-C, et al. Prediction of machining accuracy degradation of machine tools. Precis Eng (2011), doi:10.1016/j.precisioneng.2011.11.002

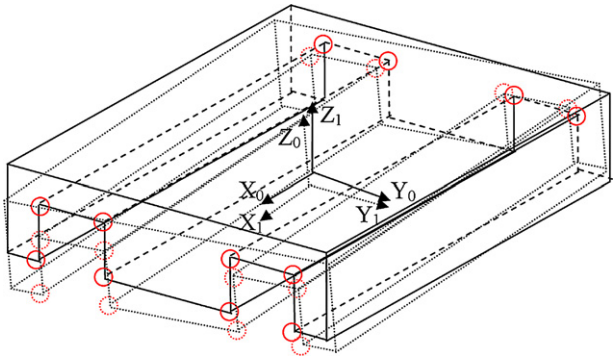

Fig. 7. Reference points of slide.

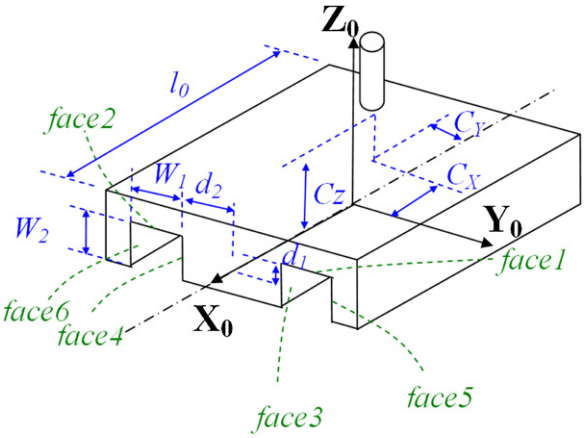

Fig. 8. Defined dimensions of the slide.

2.2. Mathematical model of the slide-guideway

The actual contact between slide and guideway in a heavy duty machine tool has more than one surface. A typical square groove type having six contact surfaces is shown in Fig. 6a, where low-friction material using Turcite B is usually applied to reduce the stick-slip and wear on sliding surfaces. The Mathematical model of the slide-guideway can be derived in a similar way as a single contact surface. First of all it is required to establish the coordinate systems. The coordinate system 0 is located at the center of the slide, which is also the center of the ballscrew nut, and coordinate systems 2–7 are located at the center of each contact surface between the slide and the guideway, as shown in Fig. 6b. It is noted that the coordinate system 1 is located at the center of the deformed slide, and twelve corner points of the slide are selected as the reference points, as shown in Fig. 7. When deformed, these reference points are embedded into the guideway, as indicated by dashed circles. Six surface equations of the slide's contact faces can be derived by these reference points.

The position of each reference point should be located in each corresponding coordinate system in order to derive the six surface equations of contact faces between the slide and the guideway. Relationships between coordinate systems can be described by the HTM operators, such as ${}^{2}T_{1}$ and ${}^{3}T_{1}$.

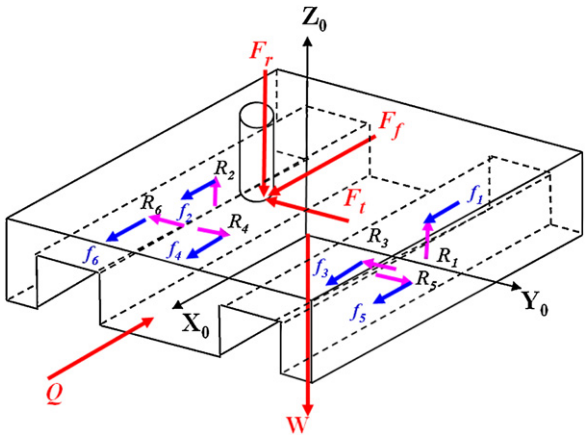

Fig. 9. Free body diagram of the slide.

The dimension and the coordinate systems of the slide are defined in Fig. 8. Its free body diagram is shown in Fig. 9. F_r, F_f, and F_t are cutting forces in corresponding X (radial), Y (feed), and Z (tangential) components respectively; C_X, C_Y, and C_Z are the corresponding X, Y, and Z components of the machining point; W is weight of slide; Q is feed force from ballscrew; R_1, R_2, R_3, R_4, R_5, and R_6 are the reaction forces on six corresponding contact surfaces, respectively; f_1, f_2, f_3, f_4, f_5, and f_6 are corresponding frictional forces on six contact surfaces. Let us define that:

M_{R1X}, M_{R2X}, M_{R3X}, M_{R4X}, M_{R5X}, and M_{R6X} are the moments of respective six reaction forces about the X_0 axis; M_{R1Y} and M_{R2Y} are the moments of two reaction forces (R_1 and R_2) about the Y_0 axis; M_{R1Z}, M_{R2Z}, M_{R3Z}, and M_{R4Z} are the moments of four reaction forces (R_1 to R_4) about the Z_0 axis; M_{f1Y}, M_{f2Y}, M_{f3Y}, M_{f4Y}, M_{f5Y}, and M_{f6Y} are moments of six frictional forces about the Y_0 axis; M_{f1Z}, M_{f2Z}, M_{f3Z}, M_{f4Z}, M_{f5Z}, and M_{f6Z} are the moments of six frictional forces about the Z_0 axis.

This analysis supposes that the slide is moving under a constant speed. At equilibrium state three force equations and three moment equations can be formulated in Eq. (13). Since these forces and moments are derived from the deformed volume which is a function of δ_{Y0}, δ_{Z0}, ε_{X0}, ε_{Y0}, ε_{Z0} and Q. Hence, the six equilibrium equations are also the functions of these variables. Six unknown variables, which are δ_{Y0}, δ_{Z0}, ε_{X0}, ε_{Y0}, ε_{Z0}, and Q, can be solved by six equations simultaneously using Newton-Raphson method.

$$\begin{aligned}
&\textstyle\sum F_X = 0 \Rightarrow f_1 + f_2 + f_3 + f_4 + f_5 + f_6 - Q + F_f = 0\\
&\textstyle\sum F_Y = 0 \Rightarrow -R_3 + R_4 + R_5 - R_6 - F_t = 0\\
&\textstyle\sum F_Z = 0 \Rightarrow R_1 + R_2 - F_r - W = 0\\
&\textstyle\sum M_X = 0 \Rightarrow M_{R1X} + M_{R2X} + M_{R3X} - M_{R4X} - M_{R5X} + M_{R6X} + F_t \cdot C_Z - F_r \cdot C_Y = 0\\
&\textstyle\sum M_Y = 0 \Rightarrow -M_{R1Y} - M_{R2Y} + M_{f1Y} + M_{f2Y} + M_{f3Y} + M_{f4Y} + M_{f5Y} + M_{f6Y} + F_r \cdot C_X + F_f \cdot C_Z = 0\\
&\textstyle\sum M_Z = 0 \Rightarrow -M_{R3Z} + M_{R4Z} + M_{R5Z} - M_{R6Z} - M_{f1Z} - M_{f2Z} - M_{f3Z} - M_{f4Z} - M_{f5Z} - M_{f6Z} - F_t \cdot C_X - F_f \cdot C_Y = 0
\end{aligned} \tag{13}$$

3. Wear of the slide-guideway and geometric errors of the slide

3.1. Wear of the slide-guideway

It is a very complex problem to calculate the wear of the slide-guideway. Not all of the reactive surfaces will be in contact during the slide sliding along the guideway. The amount of wear on different positions of the guideway is dependent on the length of the part being machined. Fig. 10 shows several different lengths of parts that are machined. In total, the central part of the guideway has the highest probability to be machined and the curve of wear can be assumed in the form of normal distribution (Gaussian function).

The mathematical model to calculate the wear of sliding guides is modified from Pronikov's model, which assumes that the contact

Please cite this article in press as: Fan K-C, et al. Prediction of machining accuracy degradation of machine tools. Precis Eng (2011), doi:10.1016/j.precisioneng.2011.11.002

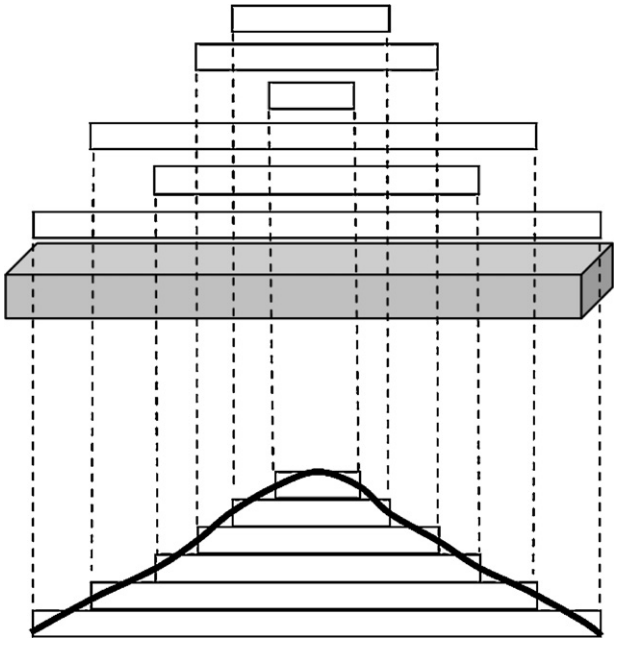

Fig. 10. Curve of wear distribution over the length of guideway.

pressure between the slide and guideway maintains constant during wear [13]. Since the non-uniform pressure distribution is due to angular errors of the slide, these errors are very small in practice, which means the slope of deformed surface containing original reference points (P1, P2 and P3) is very small. Therefore, for the ease of computation, this research assumes that the contact pressure distribution of the slide is uniform, which is the reaction force divided by the corresponding contact surface area. However, this uniform pressure pattern is varied along the guideway and is a function of the cutting position x. Based on this assumption, the slide wear will be uniform over the contact surface, while guideway wear will be a function of the cutting position x. Such a concept can be depicted by Fig. 11.

Let L be the maximum slide travel; $P(X)$ be the uniform contact pressure pattern of slide at cutting position X; $\phi(X)$ be the total sliding path distribution curve; S be the sliding path traversed by each point on the slide in the given period of time.

The contact pressure pattern $P(X)$ can be derived by curve fitting with series of pressure data which are reaction forces divided by contact area, and the reaction forces are calculated from Eq. (13).

The volume of material removed by wear is proportional to the interface pressure, sliding distance and wear coefficient. The wear curve of the slide (Us) will be flat because the contact pressure

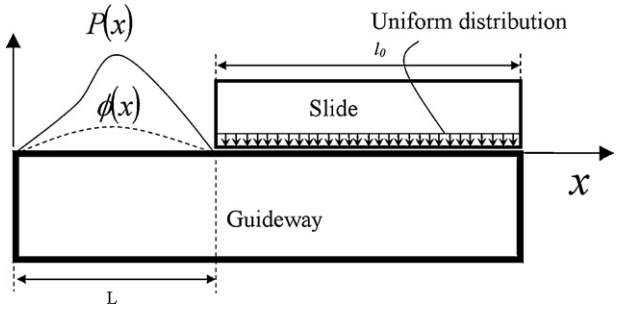

Fig. 11. Diagram for determining wear on slide-guideway.

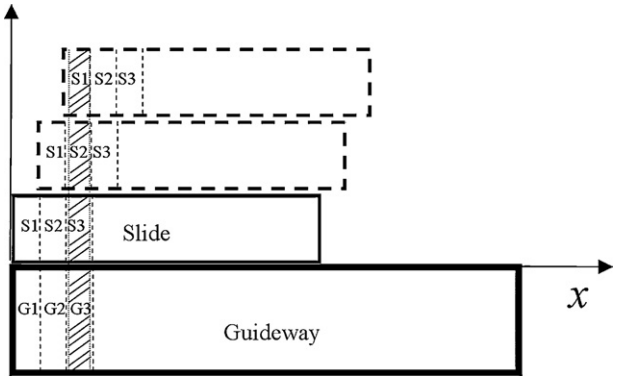

Fig. 12. Wear of guideway.

distribution is uniform, and the contact pressure is the mean of the integral of contact pressure curve $P(X)$.

$$Us = \frac{k_2 S}{L} \int_0^L P(X)dX \tag{14}$$

k_2 is the abrasive wear factor of slide material, namely Turcite B, which indicates the amount of linear wear (μm) at a specific pressure of (1 kgf/cm^2) acting over a friction path of 1 km for the given pair of materials in the given wear conditions.

The most important factor affecting the loss of accuracy of machine tool is the form of the worn surface of the guideway. The wear of guideway is a cumulative phenomenon, and not all of the reactive surfaces will be in contact during the slide sliding along the guideway. Fig. 12 shows the cumulative phenomenon of the guideway wear, where portion G3 experiences wear by contacting slide segments S1, S2 and S3. The wear at position x of the guideway is expressed by

$$Ug(x) = k_1 S \int_{l_1}^{l_2} \phi(x - X)P(x - X)dX \tag{15}$$

where k_1 is the abrasive wear factor of the guideway material, namely cast iron.

The limits of integration of Eq. (15) depend on which section the guideway is under wear, as propose by Pronikov [13]. This is shown in Table 1.

3.2. Slide geometric errors caused by guideway wear

Ekinci and Mayer [14] proposed mathematical formulae which establish analytical relations between joint kinematic and geometric errors, as shown in Fig. 13. Joint kinematic angular error and straightness error of a slide moving on a guideway with a geometric error $\Delta(X)$ are

$$\varepsilon_V(X) = \frac{\Delta(X + (l_0/2)) - \Delta(X - (l_0/2))}{l_0} \tag{16}$$

Table 1
Limits of integration [13].

L/l_0	Section	Section limits	Limits of integration	
			l_1	l_2
>1	I	$0 \leqq x \leqq l_0$	0	x
	II	$l_0 \leqq x \leqq L$	0	l_0
	III	$L \leqq x \leqq L + l_0$	$x - L$	l_0
<1	I	$0 \leqq x \leqq L$	0	x
	II	$L \leqq x \leqq l_0$	$x - L$	x
	III	$l_0 \leqq x \leqq l_0 + L$	$x - L$	l_0

Please cite this article in press as: Fan K-C, et al. Prediction of machining accuracy degradation of machine tools. Precis Eng (2011), doi:10.1016/j.precisioneng.2011.11.002

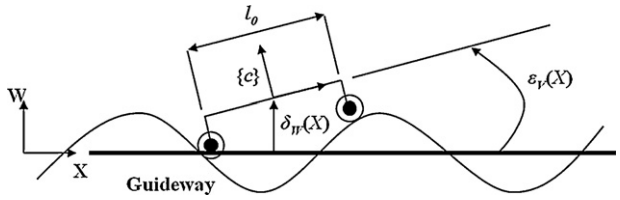

Fig. 13. slide-guideway configuration.

Table 2
Specifications of slide and guideway.

l_0 (mm)	530	d_1 (mm)	100
L_G (mm)	900	d_2 (mm)	300
W_1 (mm)	100	W (kgf)	550
W_2 (mm)	35	K (kgf/cm^2-μm)	0.274
μ	0.04	k_1 (μm-cm^2/kgf-km)	0.0191
H_1 (HRC)	52.9	k_2 (μm-cm^2/kgf-km)	0.0222
H_2 (HRC)	45.5		

Table 3
Cutting data.

F_t (kgf)	150	C_X (mm)	−185 to 185
F_f (kgf)	100	C_Y (mm)	0
F_r (kgf)	100	C_Z (mm)	200

$$\delta_W(X) = \frac{\Delta(X + (l_0/2)) - \Delta(X - (l_0/2))}{2} \tag{17}$$

This mathematic model is for only a single contact surface of guideway. In general machine tool, however, each moving axis has six contact surfaces between slide and guideway, as explained in Fig. 6. Each straightness and angular errors of the ith contact surface, denoted by $\delta_{Wi}(X)$ and $\varepsilon_{Vi}(X)$ respectively, can be calculated by Eqs. (16) and (17). The combined slide's geometric errors are then obtained from corresponding surfaces as follows.

$$\varepsilon_X(X) = \frac{\delta_{W1}(X) - \delta_{W2}(X)}{2d_2 + W_1} \tag{18}$$

$$\varepsilon_Y(X) = \frac{\varepsilon_{V1}(X) + \varepsilon_{V2}(X)}{2} \tag{19}$$

$$\varepsilon_Z(X) = \frac{\varepsilon_{V3}(X) + \varepsilon_{V4}(X) + \varepsilon_{V5}(X) + \varepsilon_{V6}(X)}{4} \tag{20}$$

$$\delta_Y(X) = \begin{cases} \dfrac{\delta_{W4}(X) + \delta_{W5}(X)}{2}, & F_t \le 0 \\ \dfrac{\delta_{W3}(X) + \delta_{W6}(X)}{2}, & F_t > 0 \end{cases} \tag{21}$$

$$\delta_Z(X) = \frac{\delta_{W1}(X) + \delta_{W2}(X)}{2} \tag{22}$$

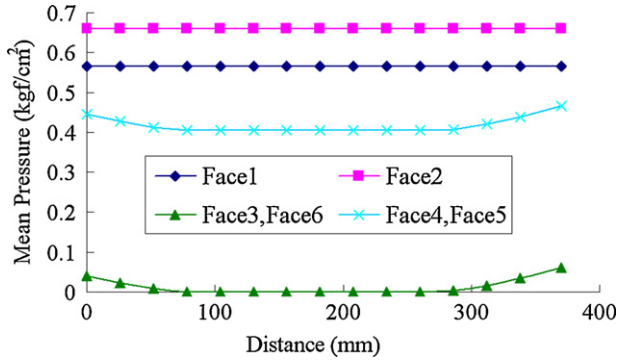

Fig. 14. Contact pressure on each surface.

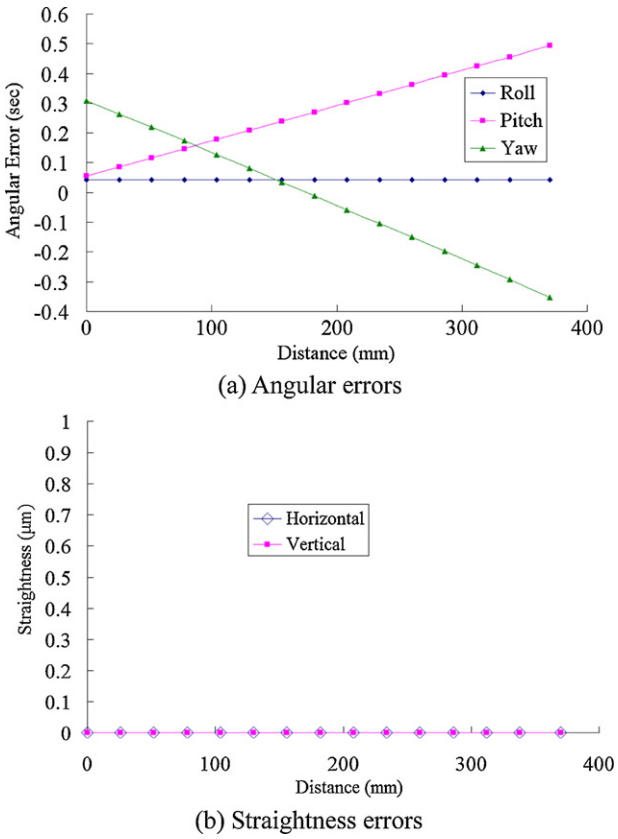

Fig. 15. Geometric errors of slide due to contact deformation of the slide-guideway, (a) angular errors and (b) straightness errors.

where $\varepsilon_X(X)$, $\varepsilon_Y(X)$ and $\varepsilon_Z(X)$ are the roll, pitch and yaw errors of the slide respectively over length x with $0 \le x \le L$; $\delta_Y(X)$ and $\delta_Z(X)$ are the horizontal and vertical straightness errors of the slide over length X with $0 \le X \le L$.

The geometric errors of the slide will be increased due to the increase of the guideway wear. The induced positioning errors, or called Abbé errors at cutting point, can be expressed by Eq. (23). These errors will grow gradually and is a function of wear distance.

$$\begin{bmatrix} E_X(X) \\ E_Y(X) \\ E_Z(X) \\ 1 \end{bmatrix} = \begin{bmatrix} 0 & -\varepsilon_Z(X) & \varepsilon_Y(X) & 0 \\ \varepsilon_Z(X) & 0 & -\varepsilon_X(X) & \delta_Y(X) \\ -\varepsilon_Y(X) & \varepsilon_X(X) & 0 & \delta_Z(X) \\ 0 & 0 & 0 & 1 \end{bmatrix} \cdot \begin{bmatrix} C_X \\ C_Y \\ C_Z \\ 1 \end{bmatrix}$$

$$= \begin{bmatrix} -\varepsilon_Z(X) \cdot C_Y + \varepsilon_Y(X) \cdot C_Z \\ \varepsilon_Z(X) \cdot C_X - \varepsilon_X(X) \cdot C_Z + \delta_Y(X) \\ -\varepsilon_Y(X) \cdot C_X + \varepsilon_X(X) \cdot C_Y + \delta_Z(X) \\ 1 \end{bmatrix} \tag{23}$$

where C_X, C_Y and C_Z are Abbé offsets from the coordinate axes to the cutting point, as given in Fig. 8.

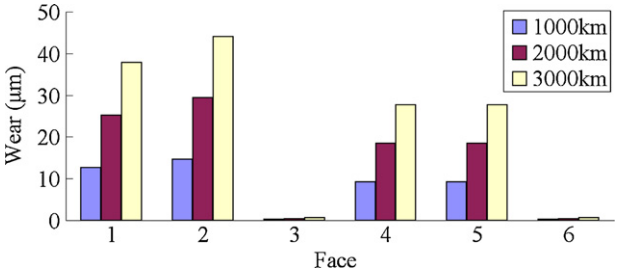

Fig. 16. Wear depth of slide.

Please cite this article in press as: Fan K-C, et al. Prediction of machining accuracy degradation of machine tools. Precis Eng (2011), doi:10.1016/j.precisioneng.2011.11.002

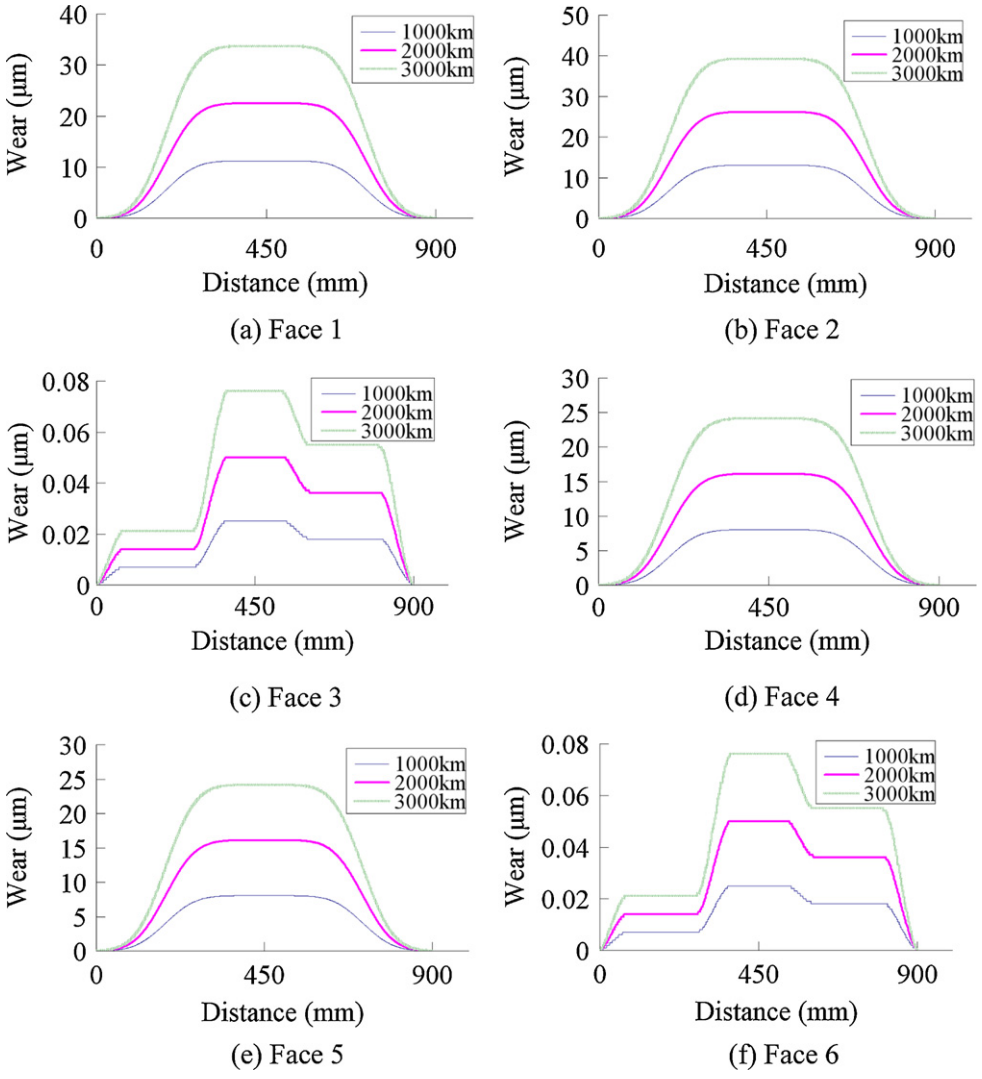

Fig. 17. Wear depth of guideway, (a) Face 1, (b) Face 2, (c) Face 3, (d) Face 4, (e) Face 5 and (f) Face 6.

4. Simulation

4.1. Parameters of slide-guideway

The dimensions of slide and guideway are provided by a machine tool builder. The dimensions of studied slide-guideway are listed in Table 2, where L_G is the length of guideway and other parameters are defined in Figs. 8 and 9. The contact deformation parameter ($K = 0.274$) in Eq. (10), the friction coefficient ($\mu = 0.04$) of Turcite B-Cast iron couple, and the wear coefficient of Turcite B ($k_2 = 0.222$) are obtained from the technical specifications of Turcite B [15].

Because the wear coefficient of cast iron coupling with Turcite B is not able to be found in any literature, we have to make the following assumption. Since the wear rate of material is related to its hardness [16], the wear coefficient of cast iron coupling with Turcite B can be estimated according to the ratio of hardness between cast iron and Turcite B. The hardness of cast iron (H_1) and the hardness of Turcite B (H_2) are listed in Table 2 [15], then the wear coefficient of cast iron (k_1) can be estimated as: $k_1 = k_2(H_2/H_1) = 0.0191$. All units are indicated in Table 2.

Table 4
Specifications of slide-guideway test bed.

l_0 (mm)	410	d_1 (mm)	68
L_G (mm)	660	d_2 (mm)	40
W_1 (mm)	40	W (kgf)	10
W_2 (mm)	25	k_1 (μm-cm^2/kgf-km)	0.49
μ	0.11	k_2 (μm-cm^2/kgf-km)	0.49

4.2. Results of simulation

Cutting data are given in Table 3. The magnitudes of cutting forces are based on the cutting conditions including feed rate, depth of cut, cutter, material, etc. [4]. This study is to predict the accuracy changes after 1000-km, 2000-km and 3000-km cutting distances.

Under known external forces acting on the slide, the contact pressure pattern $p(x)$ can be derived by curve fitting with series of pressure data which are reaction forces divided by respective contact areas, and the reaction forces are calculated from Eq. (13). The contact pressure between slide and guideway is shown in Fig. 14. Face 1 and face 2 undertake more compression than other faces because they directly bear the slide weight and axial cutting force. When the slide is in the middle area only faces 4 and 5 equally share the tangential cutting force and no pressure on faces 3 and 6. When the slide moves to both ends, the increased moment caused by the tangential cutting force will produce yaw motion of the slide that increases the contact pressure on faces 3, 4, 5 and 6.

Please cite this article in press as: Fan K-C, et al. Prediction of machining accuracy degradation of machine tools. Precis Eng (2011), doi:10.1016/j.precisioneng.2011.11.002

Cutting force, feed force and friction force applied to the slide will yield elastic deformation of its contact surface and cause geometric errors of the slide when it moves along the guideway. Fig. 15a shows that the pitch and yaw errors are caused by the moment changes because the moment arms are varied due to the change of machining point when the slide moves. There is no roll error because the contact pressures on face 1 and face 2 remain constant. The straightness plot shown in Fig. 15b indicates the slide has no lateral translation errors in vertical and horizontal directions during the traverse on the guideway. It is because the elastic deformation on corresponding faces remains constant. Compared with a previous work [4], it can be seen that the trends of simulated pitch, yaw, and roll are quite reasonable.

After a long period of cutting operation, the guideway will be worn out and becomes a concave shape in both of the vertical and horizontal planes. The slide is also worn out. The volume of material removed by wear is proportional to the interface pressure, sliding distance and wear coefficient, and the total sliding path distribution curve is considered the normal distribution. Fig. 16 shows the wear depth of the slide and Fig. 17 is the guideway. The slide has more serious wear than guideway, because the wear coefficient of slide (Turcite material) is larger than the guideway (Cast iron material) and whole contact surface of slide wears over the entire cutting distance. Contact surfaces 1 and 2 are resulted in more serious wear because they directly bear the slide's weight and the axial cutting force. In addition, the wear depth of surface 2 is larger than surface 1, because the lateral cutting force causes the moment that acts on surface 2. Surfaces 3 and 6 have the same wear depth, so are surfaces 4 and 5. However, surfaces 4 and 5 undertake more contact load, which yields to the bending of the guideway in horizontal plane. The wear on surfaces 3 and 6 can be neglected. It also shows the wear form of contact surfaces 1, 2, 4 and 5 are all symmetrical to the central point.

Fig. 18 shows the slide's three angular errors along the guideway. The roll is caused by the difference in deformation between face 1 and face 2. It remains constant because the difference is constant as shown in Fig. 17a and b. The pitch and yaw gradually grow and symmetrical to the guideway center in a form of concave shape. Again, after the wear is formed the induced pitch, yaw and roll errors are similar to the trend investigated by [4].

Fig. 19 shows that after the wear is generated, the amount of wear due to the elastic deformation of slide-guideway contact surface will result in only the lateral shift in both directions but no induced straightness error of the slide's motion.

Fig. 20 shows the induced positioning errors due to slide's geometric errors along the worn guideway. The induced positioning errors are caused by the deformed shape of the guideway surface, which will induce angular motion of the slide (or called the moving carriage). Based on the Abbe principle, this angular motion will generate positioning error at the cutting point. Since the wear forms of the 6 contact surfaces of the guideway are all symmetrical to the respective travel centers, being a concave shape, the wear induced positioning errors, will be larger at both ends.

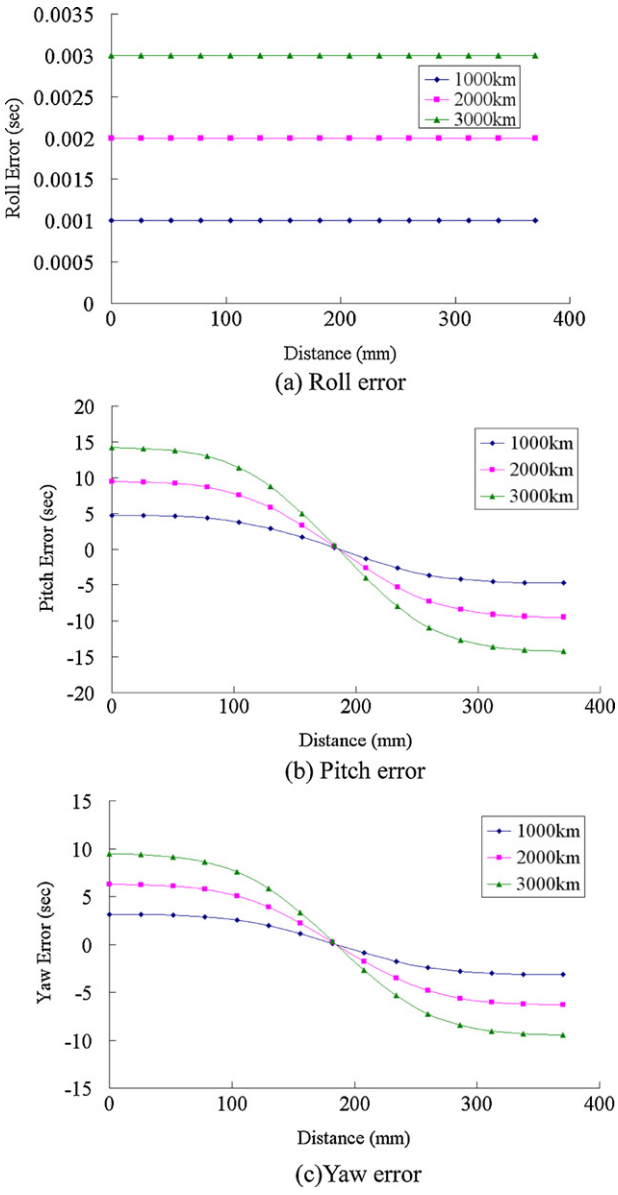

Fig. 18. Slide's angular errors due to guideway wear, (a) roll error, (b) pitch error and (c) yaw error.

5. Experiments and analysis

5.1. Experimental setup

A test bed of wear experiment on a linear stage has been built up, as shown in Fig. 21. The dimensions of studied slide-guideway are listed in Table 4, where L_G is the length of guideway, W is the weight of the slide, and other parameters are defined in Fig. 8. The materials of the slide and the guideway are both FC25 cast iron. The friction coefficient ($\mu = 0.11$) and the wear coefficients ($k_1 = 0.49$, $k_2 = 0.49$) of Cast iron-Cast iron couple, are obtained from [17]. Two air plungers applied to the slide in vertical and horizontal directions are used to simulate the cutting forces in radial and tangential directions respectively, as there are more effective to the wear of the slide's inner walls. As the maximum load of the air plunger is limited to 50 kg, we set the applied load to 34 kg by the servo valve, being a medium load cutting condition. A laser interferometer (HP 5529A) is equipped to measure the slide's lateral shift (with the straightness kit) or the angular errors along the travel (with the angular kits). The growth of wear is to be detected by the increased pitch error of the slide.

5.2. Measurement of deformation coefficients

Prior to the wear measurements, the relationship between the normal pressure (P) and the deformation (λ) of the contact surfaces can be obtained by the experiment only with the side load of Fig. 21. The lateral displacements under applied loads were measured by the HP 5529 laser straightness interferometer. Fig. 22 shows the

Please cite this article in press as: Fan K-C, et al. Prediction of machining accuracy degradation of machine tools. Precis Eng (2011), doi:10.1016/j.precisioneng.2011.11.002

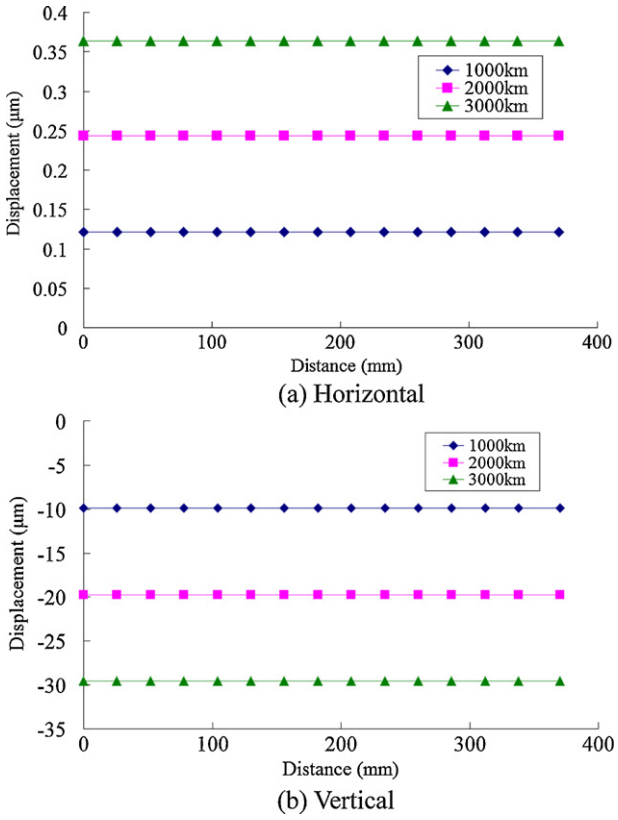

Fig. 19. The lateral shift of the slide's motion due to guideway wear, (a) horizontal and (b) vertical.

results of experiment. The coefficients (c and m) of Eq. (1) can thus be obtained from the least-squares fitting.

5.3. Experimental results, analysis and discussions

The vertical load applied to the slide will cause the pitch error of the slide during motion. This pitch error can be measured by the HP 5529 laser angular interferometer. The increased wear of the guideway can be reflected by the increased pitch errors. In order to verify the analytical solution, therefore, the pitch errors under load are firstly measured. Fig. 23 shows the comparison of experimental and simulated initial pitch errors of slide caused by a vertical load of 34 kg. The analytical pitch error (ε_{Y0}) is solved from Eq. (19). It can be seen that experimental result is quite consistent with the analysis result. Although the experimental result is slightly smaller than the analytical result, it can be assumed that at the running-in period the contact surfaces have some manufacturing errors.

The wear experiment of slide-guideway was then carried out. The vertical and horizontal loads were applied by air plungers simultaneously. The distance of each travel is 250 mm. This experiment has been conducted about 10 months with around a 5-h run per working day. The total sliding distance is accumulated to about 100 km.

In the beginning, the test bed has to be run for about 4 km of the sliding distance in order to record the initial (reference) pitch error at each traveling position. This is to avoid some possible surface irregularities of the matching pair. Fig. 24(a) shows the increased pitch errors measured at different total sliding distances relative to the reference data. It can be seen that the guideway occurs concave deformation and the maximum pitch error increase is at the end position (250 mm). Therefore, the trend of increased pitch errors at the end position was taken to analyze the wear behavior, as shown in Fig. 24(b). The wear is a function of time or sliding distance, the

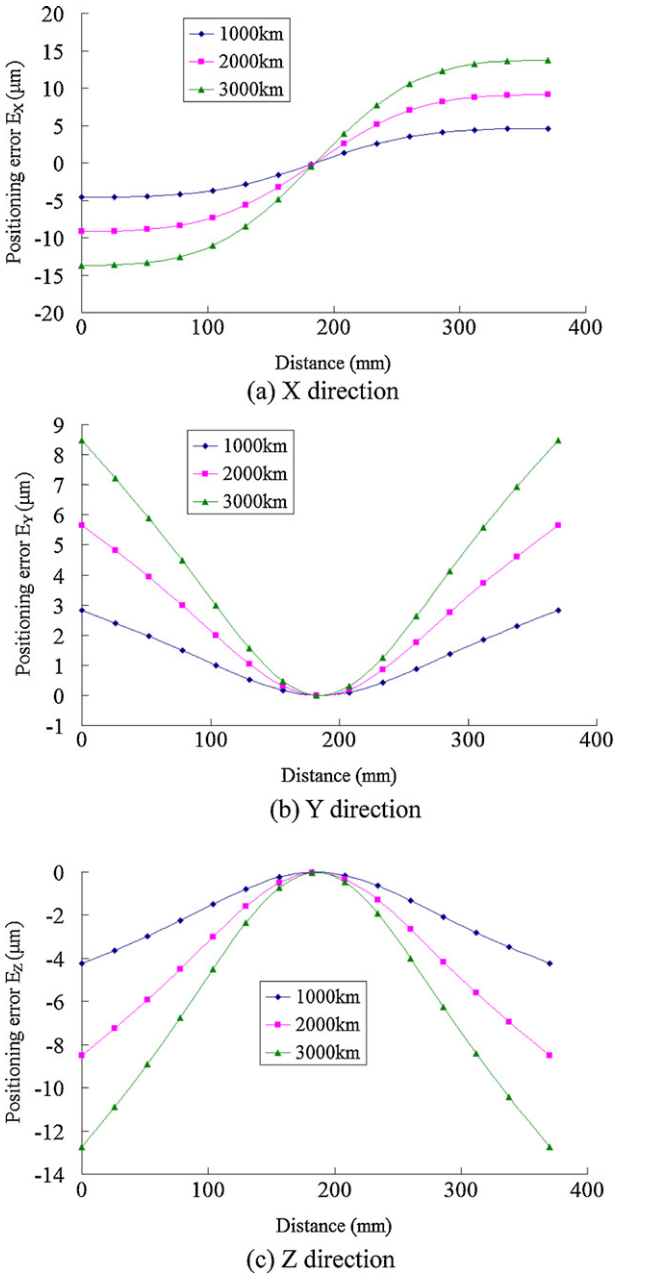

Fig. 20. The induced positioning errors due to slide's geometric errors along the worn guideway, (a) X direction, (b) Y direction and (c) Z direction.

progress of wear can be divided into three different periods, namely running-in, steady-state and breakdown [18]. It is found that at running-in period, around up to 50 km of this stage, the pitch error (same as wear) increases rapidly, although the amount is not very big, it then slows down. This wear effect can be explained that the slide-guideway contact deformation comes to steady state after a certain sliding distance. Current experiment only reaches to the steady-state wear condition.

The wear growth is a function of sliding distance [18], and the wear coefficient will change with sliding distance [19]. Fig. 24 verifies the same result. Therefore, further study on the actual wear coefficient was carried out.

The pitch error of the slide moving on the worn guideway can be calculated by Eq. (19) and is proportional to the amount of wear, which can be calculated by Eq. (15). It is also known that, from Eq. (15), the amount of wear is proportional to the wear

Please cite this article in press as: Fan K-C, et al. Prediction of machining accuracy degradation of machine tools. Precis Eng (2011), doi:10.1016/j.precisioneng.2011.11.002

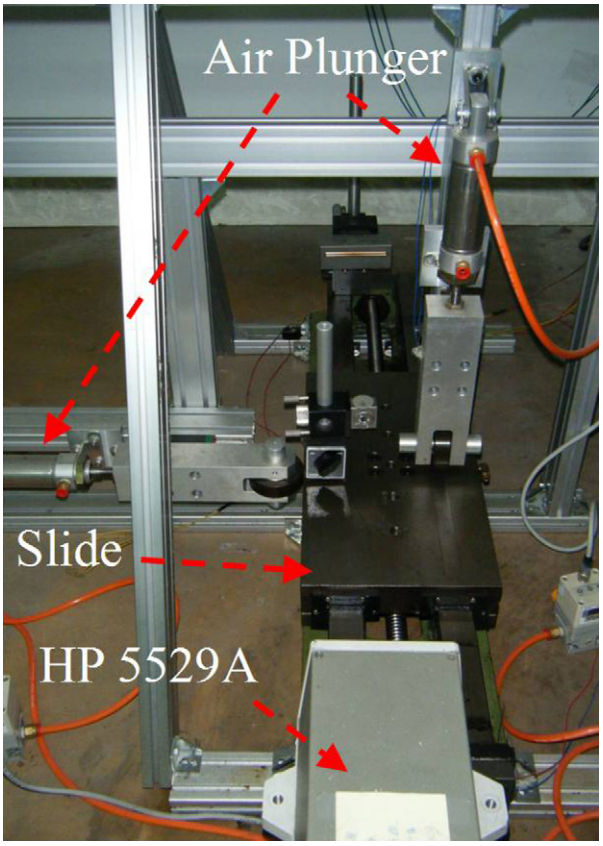

Fig. 21. Photo of test bed.

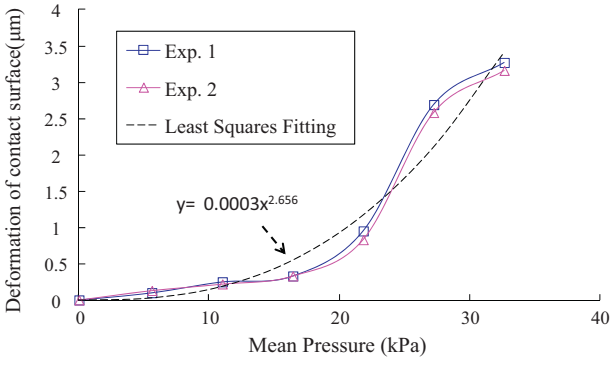

Fig. 22. Relationship between the contact pressure and the deformation.

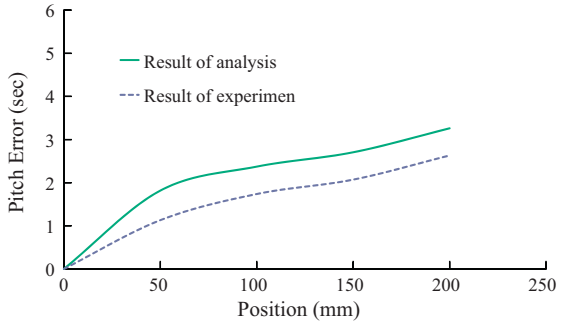

Fig. 23. Initial pitch errors of the slide due to contact deformation of slide-guideway.

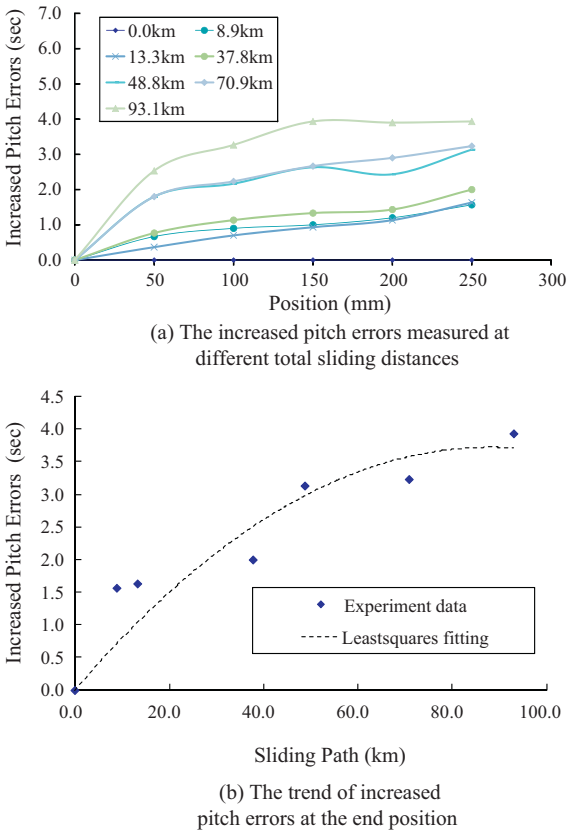

Fig. 24. The increase of pitch error due to wear: (a) the increased pitch errors measured at different total sliding distances and (b) the trend of increased pitch errors at the end position.

coefficient. Therefore, the angular error is also proportional to the wear coefficient. The empirical wear coefficient k_{exp} in this studied slide-guideway can thus be expressed as

$$\frac{\varepsilon_V(X)_{\exp}}{\varepsilon_V(X)_{analysis}} = \frac{k_{\exp}}{k_{theory}} \tag{24}$$

where k_{theory} is 0.49 obtained from [17], $\varepsilon_V(X)_{exp}$ is the measured pitch error, and $\varepsilon_V(X)_{analysis}$ is the pitch error calculated by Eq. (16).

Fig. 25 shows the pitch error changing rate with the sliding path fitted by an exponential function ($Pitch_{exp}(S)$). The analytical changing rate of pitch error is constant because k_{theory} is constant, and its value is 0.0796 obtained from Eq. (19). Therefore, the wear

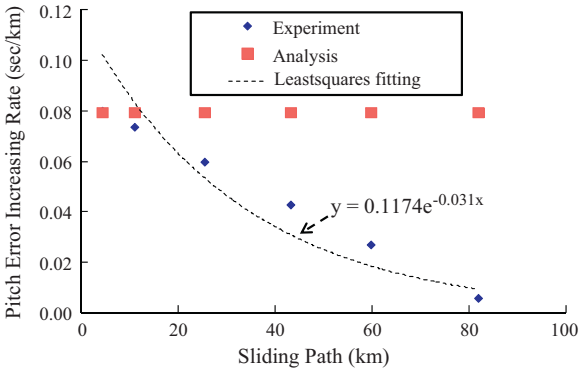

Fig. 25. Pitch error changing rate.

Please cite this article in press as: Fan K-C, et al. Prediction of machining accuracy degradation of machine tools. Precis Eng (2011), doi:10.1016/j.precisioneng.2011.11.002

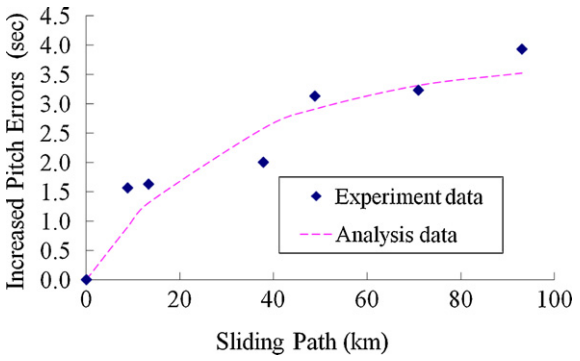

Fig. 26. Pitch error changing of slide at position 250 mm.

coefficient should be a function of sliding path ($k_{exp}(S)$) and, from Eq. (24), expressed as

$$k_{\exp}(S) = \frac{Pitch_{\exp}(S) \times 0.49}{0.0796} \tag{25}$$

Modifying the wear coefficients (k_1, k_2) from constant to the function of actual sliding distance, Fig. 26 shows the comparison of the increase of pitch errors of the slide between experimental and analytical results. It is clearly seen that they are quite matched quantitatively.

6. Conclusions

This research proposes a mathematical model for the wear analysis of the slide-guideway under cutting condition. Cutting forces press each contact surface. The reaction force at each contact face causes wear of the slide as well as the guideway and gradually increases the deformed shape of the slide-guideway. Such as deformed shape, again, increases the geometric errors, yielding to the growth positioning errors. This is the formation of accuracy degradation of machine tools. This heuristic approach forms a conceptual basis for understanding the mechanism of accuracy degradation. Computation simulation shows that given known cutting forces, dimensional parameters of the slide-guideway, and friction and wear coefficients, the geometric errors of the slide due to contact deformation of slide-guideway and the positioning errors caused by wear of the guideway after a long-term operation can all be explored. Experimental tests on a linear stage with cast iron–cast iron contact surfaces have been conducted for around 100 km sliding distance lasting 10 months. The wear growth is expressed by the increase of pitch errors, which can be measured by the laser interferometer. It is found that the wear coefficient should be modified to the function of sliding distance so that the analytical results will be consistent with the experimental results.

Acknowledgements

The authors gratefully acknowledge the financial support of this work by National Science Council and ITRI of ROC.

References

[1] Burwell JF, Strang CD. On the empirical law of adhesive wear. Journal of Applied Physics 1952;23(1):18–28.
[2] Archard JF, Hirst W. The wear of metals under unlubricated conditions. Proceedings of the Royal Society A 1956;236:397–410.
[3] Masuko M, Ito Y. Distribution of contact pressure on machine tool slideways. In: Proc. 10th int. machine tool design and research conference. 1969. p. 641–50.
[4] Furukawa Y, Moronuki N. Contact deformation of a machine tool slideway and its effect on machining accuracy. International Journal of Japanese Society of Mechanical Engineers 1987;30(263):868–74.
[5] Hinduja S. Analysis of machine tool structures by finite element method. PhD Thesis, U.M.I.S.T.; 1971.
[6] Back N. Deformations in machine tool joints. PhD Thesis, U.M.I.S.T.; 1972.
[7] Levina ZM. Calculation of contact deformations in slideways. Machines and Tooling 1965;36:8–17.
[8] Levina ZM. Research on the static stiffness of joints in machine tools. In: Proc. 8th machine tool design and research conference. 1967. p. 737–58.
[9] Tenner DG. Contact stiffness of friction slideways. Machines and Tooling 1968;39(3):3–6.
[10] Ostrovskii VI. The influence of machining methods on slideway contact stiffness. Machines and Tooling 1965;36:17–9.
[11] Back N, Burdekin M, Cowley A. Analysis of machine tool joints by the finite element method. In: Proceedings of the 14th international machine tool design and research conference. 1974.
[12] Tsukada T, Anno Y. An analysis of the elastic and plastic deformation of machined surfaces in contact. Bulletin of the JSME 1975:18.
[13] Pronikov AS. Theoretical fundamentals for calculating the wear of machine parts. Wear 1963;6(5):391–406.
[14] Ekinci TO, Mayer JRR. Relationships between straightness and angular kinematic errors in machines. International Journal of Machine Tools and Manufacture 2007;47(12–13):1997–2004.
[15] Technical Specifications Turcite-B Slydway Brochure; 2011. Aetna Plastics Corp. http://www.aetnaplastics.com/products/d/Turcite/.
[16] Karamis MB, Odabas D. A simple approach to calculation of the sliding wear coefficient for medium carbon steels. Wear 1991;151(1):23–34.
[17] Olsson H, Ukonsaari J. Wear testing and specification of hydraulic fluid in industrial applications. Tribology International 2003;36(11):835–41.
[18] Heinz K, Gahr Z. Microstructure and wear of materials. New York: Elsevier; 1987. pp. 383–384.
[19] Ma Z, Henein NA, Bryzik W, Glidewell J. Break in liner wear and piston ring assembly friction in a spark-ignited engine. Tribology Transactions 1998;41(4):497–504.

Please cite this article in press as: Fan K-C, et al. Prediction of machining accuracy degradation of machine tools. Precis Eng (2011), doi:10.1016/j.precisioneng.2011.11.002